Available online at www.sciencedirect.com
ScienceDirect
Deep-Sea Research II 55 (2008) 856–867
DEEP-SEA RESEARCH PART II
www.elsevier.com/locate/dsr2

A seasonal carbon budget for a naturally iron-fertilized bloom over the Kerguelen Plateau in the Southern Ocean

Marie Paule Jouandet[a], Stephane Blain[a,*,1], Nicolas Metzl[b], Christian Brunet[b], Thomas W. Trull[c], Ingrid Obernosterer[d,e]

[a]Aix-Marseille Université, CNRS, LOB-UMR 6535, Laboratoire d'Océanographie et de Biogéochimie, Campus de Luminy, Case 901, 13288 Marseille cedex 09, France
[b]LOCEAN-IPSL, UMR 7159, CNRS, Université P. et M. Curie, Case 100, 4, Place Jussieu, 75252 Paris Cedex 5, France
[c]Antarctic Climate and Ecosystems CRC, University of Tasmania, CSIRO Marine and Atmospheric Research, Hobart, Tas 7001, Australia
[d]Université Pierre et Marie Curie-Paris6, Laboratoire ARAGO, Avenue Fontaulé, BP44, F66650 Banyuls-sur-Mer, France
[e]CNRS, UMR7621, Laboratoire d'Océanographie Biologique de Banyuls, Avenue Fontaulé, BP44, F-66650 Banyuls-sur-Mer, France

Accepted 11 December 2007
Available online 11 April 2008

Abstract

During the Kerguelen Ocean and Plateau compared Study (KEOPS, January–February 2005), a high-resolution distribution of surface fugacity of carbon dioxide (fCO_2) was obtained from underway measurements. The stations in the core of the naturally iron-fertilized bloom were characterized by low fCO_2 (311 ± 8 μatm) compared to the atmosphere, thus representing a large CO_2 sink. This contrasted with stations typical of high-nutrient low-chlorophyll (HNLC) conditions where the surface water was roughly in equilibrium with the atmosphere ($fCO_2 = 372 \pm 5$ μatm). The vertical distribution of dissolved inorganic carbon (DIC) also was obtained at stations within and outside the bloom. Based on this data set, we constructed a carbon budget for the mixed layer that allowed us to determine the seasonal net community production (NCP_{season}) and the seasonal carbon export in two contrasting environments. The robustness of the approach and the errors also were estimated. The NCP_{season} in the core of the bloom was 6.6 ± 2.2 mol m^{-2}, typical of productive areas of the Southern Ocean. At the HNLC station the NCP_{season} was 3 times lower than in the bloom. Our estimate of the daily net community production (NCP_{daily}) within the bloom compares well with shipboard measurements of NCP. The NCP_{daily} obtained above the Kerguelen Plateau was of the same order as the estimates from Southern Ocean artificial iron-fertilization experiments (SOIREE and EisenEx). The seasonal carbon export was derived from NCP_{season} after subtraction of the seasonal accumulation of particulate and dissolved organic carbon. In the bloom, the carbon export (5.4 ± 1.9 mol m^{-2}) was 3-fold higher than at the HNLC station (1.7 ± 0.4 mol m^{-2}). Comparison of our results to artificial iron-fertilization experiments shows that the biological pump is enhanced by natural iron fertilization.

Keywords: Natural iron fertilization; Carbon budget; Carbon fluxes

1. Introduction

The Southern Ocean is a key player in the global carbon cycle. There is accumulating evidence from modelling work, paleoceanographic studies, and field investigations that the Southern Ocean played a crucial role in setting the partial pressure of CO_2 in the atmosphere during glacial and pre-industrial times (Bopp et al., 2003; Marinov et al., 2006; Watson and Naveiro Garabato, 2006; Aumont and Bopp, 2006) by controlling the global biological production (Sarmiento et al., 2004). The Southern Ocean is also thought to play an important role by pumping anthropogenic CO_2 from the atmosphere (Sabine and Gruber, 2005; Lo Monaco et al., 2005). However, the detailed

*Corresponding author. Tel.: +33 4 68 88 73 44; fax: +33 4 68 88 73 95.
E-mail addresses: marie-paule.jouandet@univmed.fr (M.P. Jouandet), stephane.blain@obs-banyuls.fr (S. Blain).
[1]Present address. UPMC, Univ Paris 06, UMR CNRS 7621, BP 44, 66650 Banyuls-sur-mer, France.

0967-0645/$ - see front matter © 2008 Elsevier Ltd. All rights reserved.
doi:10.1016/j.dsr2.2007.12.037

mechanisms driving these important global processes are still partly puzzling. This is particularly the case for the functioning of the biological pump.

The large amount of unused nutrients in the Southern Ocean results from an inefficient biological pump. The limitation of phytoplankton production by iron is now recognized as the most convincing explanation of the high-nutrient low-chlorophyll (HNLC) conditions prevailing in the Southern Ocean. This has been clearly demonstrated by deliberate iron-enrichment experiments carried out in different provinces: SOIREE in the Indian sector (Boyd et al., 2000), SOFex in the Pacific sector (Coale et al., 2004), and EisenEx in the Atlantic sector (Smetacek, 2001; Bozec et al., 2004). All these experiments resulted in an increase in phytoplankton biomass dominated by diatoms, and in a strong decrease of the partial pressure of CO_2 (pCO_2) in surface waters of the fertilized patch (de Baar et al., 2005). During SOIREE and EisenEx, however, no detectable increase in carbon export was observed within the patch as compared to outside (Charette and Buesseler, 2000; Nodder et al., 2001). During SOFex, a high-resolution study of the ^{234}Th deficit in the water column revealed an excess of carbon export ($7\,mmol\,m^{-2}\,d^{-1}$) below the fertilized patch as compared to the natural background (Buesseler et al., 2004). Carbon export in the artificial iron enrichments may be underestimated as a result of the short-term (weeks) experiments and the entrainment of surrounding HNLC waters into the iron-enriched bloom. Thus an extrapolation of these experiments to longer time scales (months) is difficult (Boyd, 2004). Investigations in oceanic regions suspected to be naturally enriched in iron were also carried out (De Baar et al., 1995; Sedwick and Di Tullio, 1997; Blain et al., 2001; Aristegui et al., 2002). However, none of them directly addressed the carbon export issue.

The KErguelen Ocean and Plateau compared Study (KEOPS) was designed to study the impact of natural iron fertilization on the biology and the biogeochemistry of the surface water of the Southern Ocean (Blain et al., 2007). The occurrence of a deep source of dissolved iron (DFe) above the plateau supported the massive three-month bloom detected by satellite. By comparison with the surrounding HNLC waters, the fertilization of the surface water of the Plateau resulted from both a higher winter stocks and an enhancement of on-going supply by diapycnal mixing of DFe (Blain et al., 2008).

In this paper we present the carbon budgets for the mixed layer for contrasting stations representative of the fertilized bloom and the HNLC ocean. From these budgets we derive the seasonal net community production (NCP) and the carbon export below the mixed layer. Our results are compared with other estimates of these terms obtained by different approaches during KEOPS. We also compare our findings with carbon budgets based on a similar approach in different parts of the Southern Ocean (Karl et al., 1991; Ishii et al., 1998, 2002; Rubin et al., 1998; Sweeney et al., 2000; Jabaud-Jan et al., 2004; Metzl et al., 2006) and with the carbon budgets constructed for SOIREE and EisenEx (Bakker et al., 2005).

2. Materials and methods

2.1. Sampling strategy and analytical methods

The KEOPS cruise took place from 19 January to 13 February 2005. Near-real-time satellite images (composite of MODIS and MERIS images provided by ACRI Co) were used to determine the position of the stations. Three transects (A, B, C) of 11 stations each were carried out (Fig. 1). Station A3 (50°38′S, 72°05′E) was visited five times during the cruise and is considered to be the bloom reference station. Station C11 (51°39′S, 78°00′E) was visited twice during the cruise and is considered to be the HNLC reference station (Blain et al., 2008). Hydrological parameters of the water column were measured using a CTD (Seabird SBE19 +) mounted on a rosette equipped with 24 General Oceanics 12-L bottles. The wind speed was continuously measured aboard at 17 m and corrected to obtain the wind speed at 10 m according the formulation given by Gill (1982).

During the cruise, underway measurements of sea surface fugacity of CO_2 (fCO_2), dissolved inorganic carbon (DIC) and total alkalinity (TA) were performed using the instrumentations maintained aboard the R.V. *Marion-Dufresne* as part of the long-term observational program OISO (Metzl et al., 2006). Sea-surface water is continuously pumped at about 5 m and feeds separately the DIC/TA and fCO_2 cells. For fCO_2, seawater is equilibrated using a "thin film" type equilibrator thermostated with surface sea water (Poisson et al., 1993). A closed loop of about 100 ml of air circulates at a counter current in the equilibrator, dried in an automatic cold trap system (−35 °C), and measured with a non-dispersive infrared analyzer (NDIR, Siemens Ultramat 5F). Standard gases for calibration (280.0, 360.2, 470.4 and 502.0 ppm) and atmospheric CO_2 were measured every 7 h.

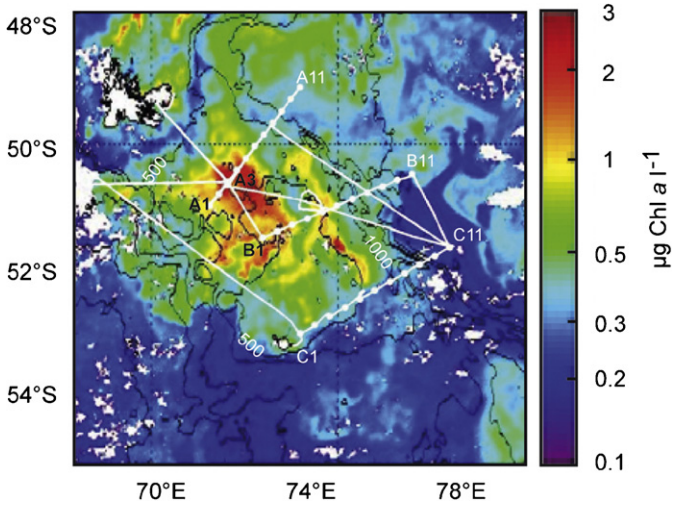

Fig. 1. Satellite images of the bloom during the KEOPS cruise. The track of the cruise (white line, the position of the stations (white dots) and the bathymetry (black lines) are shown.

To correct measurements to *in situ* data, we used polynomials given by Weiss and Price (1980) for vapor pressure and by Copin-Montégut (1988, 1989) for temperature (temperature in the equilibrium cell was on average 1 °C warmer than SST). Based on several cruises conducted with the same instrumentation (Jabaud-Jan et al., 2004; Metzl et al., 2006) and international air–sea intercomparison (Koertzinger et al., 2000), the oceanic fCO_2 data are accurate to about ± 1 µatm. Atmospheric CO_2 measurements also helped controlling the quality of the fCO_2 data (e.g., NDIR drift).

Underway (surface water) and discrete (water column) DIC and TA measurements were carried out using a technique based on the potentiometric method (Edmond, 1970) described by Jabaud-Jan et al. (2004). For semi-continuous surface measurements (3 per hour), the system is automatized for sampling seawater, transferring it into the thermostated closed cell (around 20 °C) and start the titration. The DIC accuracy ($2.2 \pm 0.8\,\mu mol\,kg^{-1}$) is based on Certified Reference Material (CRMs, Batch #62, 64 and 65) provided by Pr. A. Dickson (SIO, University of California). The DIC reproducibility estimated from 34 replicate analyses of surface and deep samples (mean difference) was 2.1 (± 1.9) $\mu mol\,kg^{-1}$.

Particulate organic carbon (POC) concentrations were obtained according to a high-temperature combustion coupled with mass spectrometer. Analytical precision was 10% (Raimbault, pers. comm.).

Dissolved organic carbon (DOC) concentrations ;were determined using the high-temperature combustion ;method with a Shimadzu TOC-V-CSH analyzer (Benner and Strom, 1993). One hundred microliter of sample were injected in triplicate and the analytical precision was ~2%.

2.2. Sea surface distribution of DIC and fCO_2 and station selection

The sea-surface distributions of fCO_2 and DIC were inferred from the high-resolution underway measurement of fCO_2 (12 per hour) and DIC (3 per hour) in surface waters (Fig. 2). At stations A1, A3, B1 and B3, located in the core of the bloom, the mean fCO_2 was 311 ± 8 µatm and the mean DIC was $2114 \pm 8\,\mu mol\,kg^{-1}$. The minimum of fCO_2 (301 µatm) was measured at station A3 (24 January) where DIC was $2104\,\mu mol\,kg^{-1}$. Outside the bloom, at stations B7, B9, C3, C5, C7, C9 and C11, the mean fCO_2 and DIC was 372 ± 5 µatm and $2134 \pm 6\,\mu mol\,kg^{-1}$, respectively. The highest values of fCO_2 (378 µatm) and DIC ($2156\,\mu mol\,kg^{-1}$) were measured at station C11. This emphasizes the difference between the HNLC C11 site, where the seawater fCO_2 was higher than in the atmosphere (fCO_{2air}), and the bloom A3 site where fCO_2 was 71.3 µatm lower than fCO_{2air}. The stations A3 and C11 were clearly representative for the bloom and HNLC conditions, respectively, and were also the most documented during the cruise (Blain et al., 2007). We therefore selected these two contrasting stations to build the carbon budgets and to estimate the impact of natural iron fertilization on carbon export on the seasonal scale.

2.3. Seasonal carbon budget

The construction of the seasonal carbon budgets relies on the stocks and fluxes measured during the cruise and also on the equations and the assumptions that are described in the following paragraphs.

2.3.1. Seasonal depletion of DIC

The seasonal depletion of DIC (ΔC_{sdep}) is the difference between the concentrations of DIC in the mixed layer during winter (DIC_{winter}) and the concentrations of DIC in the summer mixed layer (DIC_{summer}). The concentrations of DIC were normalized to the salinity of 34. Depth-integrated seasonal depletion of DIC was given by the following equation:

$$\Delta C_{sdep} = \int_0^z \Delta DIC\,\rho(z)\,dz = (DIC_{winter} - DIC_{summer}) \times \rho_{ML\ summer} z_{ML\ summer}. \quad (1)$$

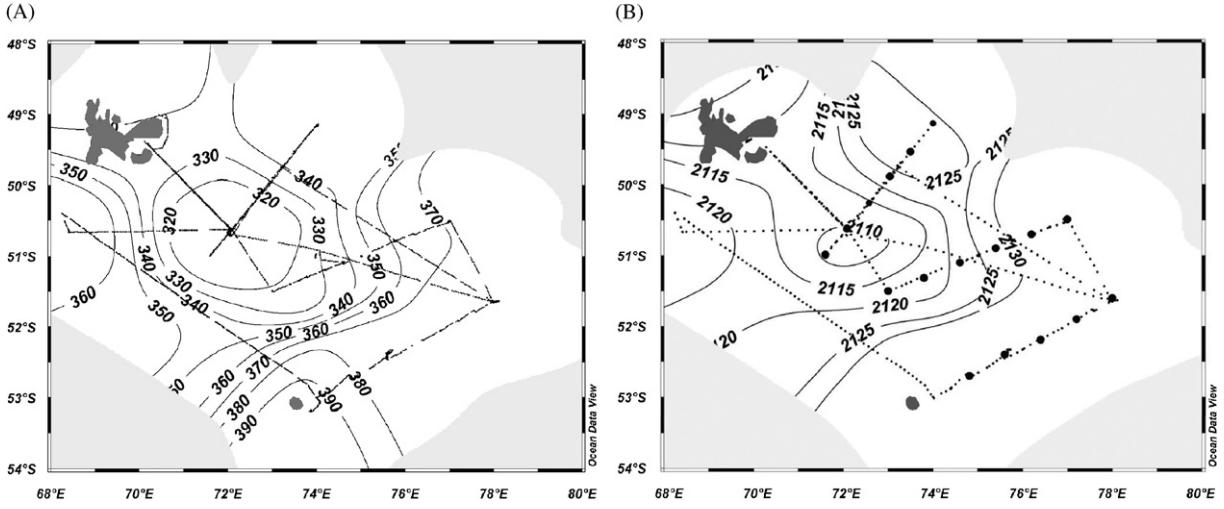

Fig. 2. Horizontal surface distributions of fCO_2 (µatm) (A) and DIC ($\mu mol\,kg^{-1}$) (B). The doted line denotes the track of the ship. Filled black circles denote the positions of the stations.

The depth of the mixed layer ($z_{MLsummer}$) was defined as the depth where the potential density differs by 2% from the surface value (Price et al., 1978). $\rho_{MLsummer}$ is the mean density of the summer mixed layer. DIC_{summer} is the mean concentration of DIC in the summer mixed layer (ML_{summer}).

In previous studies carried out in the Southern Ocean (Jennings et al., 1984; Ishii et al., 1998, 2002; Rubin et al., 1998) and in the Western Subartic North Pacific (Midorikawa et al., 2002), DIC_{winter} was estimated from the concentration of DIC at the depth of the temperature minimum considered to be representative of the Winter Water (WW) (see Appendix A). The same approach was used in this work, because the temperature minimum was clearly identified in the studied area (Fig. 3). The robustness of this approach is discussed in Appendix A.

2.3.2. Air–sea CO_2 exchange

The flux across the air–sea interface (F_{atm}) was determined with the empirical equation:

$$F_{atm} = kK_0\Delta fCO_2 = kK_0(fCO_{2\,air} - fCO_{2\,water}) \quad (2)$$

ΔfCO_2 (μatm) is the difference between sea-surface and atmospheric fCO_2. The solubility of CO_2 in sea water (K_0 in $mol\,kg^{-1}\,atm^{-1}$) was computed using the equation from Weiss (1974). The molar fraction of CO_2 in the air measured during the cruise was 375.1 ± 0.5 ppm ($fCO_2 = 372.3 \pm 0.5$ μatm). This value is similar to the monthly mean derived from hourly continuous measurements in the Southern Indian Ocean (i.e. 375.2 ± 0.5 ppm in January 2005 at Amsterdam Station, 37°57′S–77°32′E, M. Ramonet, LSCE-IPSL, pers. comm.). The transfer velocity k ($cm\,h^{-1}$) was calculated following the equations of Wanninkhof and Mc Gillis (1999, hereinafter WM99) and Nightingale et al. (2000, hereinafter N2000) with wind speeds measured continuously (every minute) during the cruise. Wind speed intensity ranged from 0.3 to 28 $m\,s^{-1}$ (with a mean value of 11.5 ± 4 $m\,s^{-1}$, $n = 27\,000$) as a result of the succession of storms and calm weather conditions. We chose WM99 and N2000 parametrizations because they differ considerably and provide reasonable upper and lower limits for the atmospheric flux for the range of wind speeds measured during KEOPS.

2.3.3. Vertical diffusive flux of DIC

The vertical profiles of DIC (Fig. 3B) show that the concentrations increased linearly between 80 and 150 m. The vertical diffusive fluxes at the base of the ML_{summer} were calculated using

$$F_{vert} = K_z\,\mathrm{grad}\,DIC_{80-150\,m} = \frac{K_z(DIC_{150} - DIC_{80})}{70} \quad (3)$$

The vertical diffusivity for the depth stratum (80–150 m) were $3.0 \pm 1.5 \times 10^{-4}$ and $3.8 \pm 3.8 \times 10^{-4}$ $m^2\,s^{-1}$ at A3 and C11, respectively (Park et al., 2008).

2.3.4. Horizontal diffusive flux of DIC

To estimate the supply of DIC to the bloom by exchange with the relatively DIC-rich surrounding surface waters we applied a simple diffusion model. The model approximates the bloom as a circular area of 200 km diameter (compare Fig. 2) that exchanges DIC with its surroundings as governed by a horizontal diffusion coefficient K_y. Throughout the area of the bloom DIC is removed at a fixed rate, J. The boundary conditions are a fixed exterior concentration at the bloom periphery and no horizontal gradient of DIC concentration at the center of the bloom. Thus the DIC mass balance is described by radial diffusion in a cylinder with a fixed sink distributed over the bloom:

$$\frac{dC}{dt} = K_y\left[\frac{d^2C}{dr^2} + \frac{1}{r}\frac{dC}{dr}\right] + J \quad (4)$$

which was solved using the spatially centered finite-difference tridiagonal matrix method (e.g., Roache, 1976).

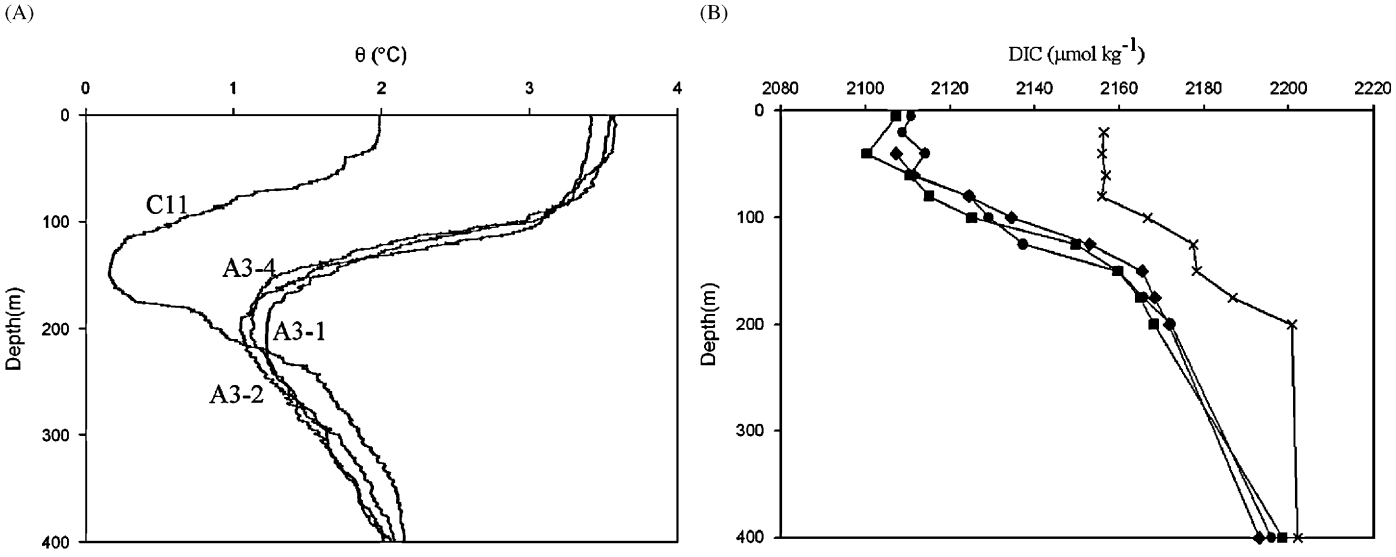

Fig. 3. Vertical profiles of temperature (A) and DIC (B) for the different visits at A3 (18 January: closed circle; 23 January: filled square; 4 February: filled diamond) and C11 (cross).

For a given diffusivity K_y and external DIC concentration, the value of the sink J sufficient to produce the observed DIC concentrations at the bloom center was estimated by an iterative procedure. For the late summer observations obtained during KEOPS (exterior DIC of 2156 μM based on the C11 HNLC station, and bloom interior DIC of 2110 μM based on the A3 bloom station; Table 1), the additional sink (above that of the net effects of air–sea exchange and export) required to balance the horizontal diffusive supply was 6.5 mmol DIC $m^{-2} d^{-1}$ for a K_y estimate of 250 $m^2 s^{-1}$ (Stammer, 1997). This estimate of K_y is based on global maps of mean sea-level height variability as observed by satellites, and higher values of 500 or even 1000 $m^2 s^{-1}$ may apply in periods of greater eddy activity. These higher diffusivities suggest correspondingly higher sinks of 13 and 26 mmol DIC $m^{-2} d^{-1}$, respectively. These sinks are expressed in terms of m^2 of horizontal surface area, i.e. they are the equivalent fluxes, F_{hor}, that would have to be removed vertically through each m^2 of surface to counteract the horizontal supply of DIC and thereby maintain the observed DIC concentrations within the bloom.

2.3.5. POC and DOC accumulation in the surface mixed layer

The seasonal accumulation of POC (Eq. (5)) and DOC (Eq. (6)) in the mixed layer is the difference between the integrated stocks in the winter and summer mixed layer.

$$\Delta POC = (POC_{summer} - POC_{winter}) z_{ML\ summer} \quad (5)$$

$$\Delta DOC = (DOC_{summer} - DOC_{winter}) z_{ML\ summer} \quad (6)$$

Table 1
Mean and standard deviations on basic terms of the carbon budget

	A3	C11
DIC_{winter} (μmol kg^{-1})[a]	2171 ± 2	2178 ± 2
DIC_{summer} (μmol kg^{-1})[a]	2110 ± 6	2156 ± 2
$z_{Mlsummer}$ (m)[b]	70 ± 20	68 ± 13
grad $DIC_{80-150\,m}$ (mmol m^{-3})[d]	0.56 ± 0.1	0.32
k[e]	7.72 ± 6.76	7.35 ± 6.4
POC_{summer} (μM)[a]	13.2 ± 1.8	5.39 ± 1.63
DOC_{summer} (μM)[a]	48.7 ± 3	–
K_z ($m^2 s^{-1}$)[d]	$3.10^{-4} \pm 1.52 \times 10^{-4}$	$3.8.10^{-4} \pm 2.34 \times 10^{-4}$
T (days)[c]	90 ± 27	90 ± 27
F_{hor} (mmol $m^{-2} d^{-1}$)[g]	6.5 ± 6.5	–
ΔC_{sdep} (mmol m^{-2})[f]	4405 ± 1432	1535 ± 364
F_{atm} (mmol $m^{-2} d^{-1}$)[f]	27.6 ± 24.51	−2.66 ± 2.28
F_{vert} (mmol $m^{-2} d^{-1}$)[f]	14.29 ± 8.99	10.51 ± 5.14

[a]Mean values between A3-1, A3-2, A3-4 ($n = 3$).
[b]Mean value on the whole of CTD for A3 ($n = 40$) and C11 ($n = 14$).
[c]Mean value was estimated by extraction of Chla satellital data, uncertainty was determined subjectively.
[d]K_z was estimated on 16 CTD ($n = 16$) at A3 and 8 at C11 ($n = 8$).
[e]k is an average between WM99 and N2000 parametrization for each wind speed registered.
[f]Calculated by the programm.
[g]Because gradient between A3 and surrounding waters was very low we could not compute any horizontal flux.

The summer concentrations were measured during the cruise (no DOC data are available at C11, Table 1). The POC winter concentration for both stations was estimated from a previous study northeast of the Kerguelen Plateau where waters were characterized by low primary productivity ($POC_{winter} = 5$ μM) (Descolas-Gros and Mayzaud, 1997). For A3 DOC_{winter} is the DOC concentration at the depth of the temperature minimum (70 μM).

3. Results and discussion

3.1. Vertical distribution

For all stations occupied during the cruise, vertical profiles of temperature revealed the existence of a subsurface minimum characterizing the winter water layer. This is typical for waters located south of the polar front in the Southern Ocean. The depth of the temperature minimum was observed at 200 m at A3 and at 150 m at C11 (Fig. 3A). Although the temperature minimum was lower at C11 (0.17 °C, $n = 1$) than at A3 (1.14 ± 0.09 °C; $n = 3$) the DIC concentrations in the WW were about the same at both stations. At A3, the mean concentration of DIC in the WW was 2171 ± 2 μmol kg^{-1} ($n = 3$) (Table 1) with very small differences between the successive visits at A3 (Fig. 3B). At C11, the concentration of DIC in the WW was slightly higher, 2178 ± 2 μmol kg^{-1}. This is consistent with the usual latitudinal gradient observed in this region (Jabaud-Jan et al., 2004). However, this difference is small compared to the large horizontal gradient of DIC existing in the surface mixed layer at the end of summer. The DIC concentration was, on average, 46 μmol kg^{-1} lower at A3 than at C11.

3.2. Seasonal NCP

NCP is the difference between net primary production and heterotrophic respiration (Williams, 1993). On the seasonal scale, NCP (NCP_{season}) is equal to the net consumption of DIC in the surface mixed layer corrected from vertical, horizontal and atmospheric DIC inputs

$$NCP_{season} = \Delta C_{sdep} + \Delta C_{atm} + \Delta C_{vert} + \Delta C_{hor} \quad (7)$$

with ΔC_{sdep} as previously defined in Eq. (1),

$$\Delta C_{atm} = \int_{t_0}^{t_{bloom}} k\, K_0 (fCO_{2\,air} - fCO_{2\,water}) \times dt = \frac{F_{atm} \Delta t_{bloom}}{2} \quad (8)$$

$$\Delta C_{vert} = \int_{t_0}^{t_{bloom}} K_z\, \mathrm{grad}\, DIC_{80-150\,m} \times dt = \frac{F_{vert} \Delta t_{bloom}}{2}, \quad (9)$$

$$\Delta C_{hor} = \int_{t_0}^{t_{bloom}} Fhor\, dt = \frac{F_{hor} \Delta t_{bloom}}{2}. \quad (10)$$

The integration of the short terms fluxes F_{atm} (Eq. (2)), F_{vert} (Eq. (3)) and F_{hor} over the entire season requires several assumptions. First, the duration of the bloom ($\Delta t_{bloom} = 90$ d) was estimated from the temporal change in Chl-*a* in surface waters inferred from satellite images (Blain et al., 2007). Secondly, for the integration of F_{atm} (Eq. (8)), we assumed that fCO_{2air} was constant over time and that the wind speed measured during KEOPS prevailed also for the rest of the season (mid November–mid January). This hypothesis is supported by the wind speed derived from QuickSCAT data for the period extending from 15 November to 15 February in the KEOPS zone (49–55°S, 70–78°E). The rate of decrease of fCO_{2water} is related to the rate of decrease of DIC in the mixed layer as well as to the seasonal warming of the surface water. Thirdly, we make the assumption that before the bloom the surface seawater was in equilibrium with the atmosphere ($fCO_{2water} = fCO_{2air}$) (Jabaud-Jan et al., 2004; Metzl et al., 2006) and that during the bloom, fCO_{2water} and DIC were decreasing linearly with time. Finally, for the integration of F_{vert} (Eq. (9)) and F_{hor} (Eq. (10)) we assume that K_z and K_y were constant over time. This is justified considering that, in the Kerguelen area, the vertical diffusive mixing is largely driven by tides (Park et al., 2008) and that the mean wind speed did not change dramatically over the season (see above). As already done for the integration of F_{atm}, we assumed that the vertical and horizontal gradients of DIC were built-up linearly during the season. The mean NCP_{season} and the associated uncertainties were computed from individual errors of the basic terms of the carbon budget (Table 1) using Monte Carlo simulations (Appendix B).

At A3, the mean NCP_{season} of 6.6 ± 2.2 mol m^{-2} was 3.5-fold higher than at C11 (1.9 ± 0.4 mol m^{-2}). The NCP_{season} determined within the bloom above the Kerguelen Plateau was quite similar to the NCP_{season} computed for other productive areas of the Southern Ocean such as coastal zones in the Ross Sea (7.3 ± 2.2 mol m^{-2}, Sweeney et al., 2000), in the seasonal ice zone of the Indian Ocean (4 ± 0.5 mol m^{-2}, Ishii et al., 1998) and in the Western Brandsfield Strait (8.41 mol m^{-2}, Karl et al., 1991). Similarly to the surface waters of the Kerguelen Plateau, all these regions are very likely naturally fertilized by iron, by different mechanisms such as upwelling of iron-rich deep water, lateral advection of lithogenic material from the continental shelf, and release of DFe from ice melting.

3.3. Daily NCP

During the cruise, NCP was determined by measuring the evolution of DIC and O_2 during 24-h deck incubations (Lefèvre et al., 2008). The highest NCP of 109 ± 44 mmol m^{-2} d^{-1} was measured during the first visit at A3, and it decreased to 29 mmol m^{-2} d^{-1} during the following visits, indicating the decline of the bloom. To make a comparison possible, we have computed the mean daily NCP (NCP_{daily}) according to the following:

$$NCP_{daily} = \frac{\Delta C_{sdep}}{\Delta t_{bloom}} + F_{atm} + F_{vert} + F_{hor}. \quad (11)$$

At A3, NCP_{daily} (99 ± 37 mmol m^{-2} d^{-1}) was equivalent to the value determined from short-term incubation. This good agreement suggests that the NCP measured during the cruise was very likely on the same order of magnitude during the month that preceded the cruise, a finding that is consistent with the high biomass observed above the Kerguelen plateau by satellite images. NCP_{daily} excess between A3 and C11 was of 74 ± 36 mmol m^{-2} d^{-1} and close to the value (100 mmol m^{-2} d^{-1}) determined by Lefèvre et al. (2008). The good agreement between both approaches also reinforces the validity of the assumptions made in the construction of the budgets.

3.4. Comparison to artificial iron enrichment experiments

The decrease of fCO_2 induced by the bloom above the Kerguelen Plateau was the highest ever observed for HNLC waters in the Indian sector of the Permanent Open Ocean Zone (POOZ) (Jabaud-Jan et al., 2004). During the nineties, studies conducted south of Kerguelen Island (Poisson et al., 1993; Metzl et al., 1995, data available at CDIAC Carbon Dioxide Information Analysis Center) also report large fCO_2 gradients (up to -90 µatm) associated with the Kerguelen bloom and thus confirm that the CO_2 sink is a recurrent feature in this area during austral summer.

The decrease of fCO_2 within the Kerguelen bloom is 2 fold higher than those measured during artificial iron enrichment experiments (Fig. 4). During KEOPS, the surface water temperature and the depth of the mixed layer (Fig. 4) were in the same range as observed during artificial iron-fertilization experiments performed in the Southern Ocean. The increase in phytoplankton biomass and primary production upon iron fertilization was also comparable among these studies. These parameters thus cannot be invoked to explain the difference in ΔfCO_2. fCO_2 and DIC are integrative measurements over time; thus the longer the duration of the bloom the more important is the CO_2 sink. It is therefore mainly the longer duration of the natural bloom, i.e. 3 months above the Kerguelen Plateau, compared to the short period of observations of artificial blooms (i.e. few weeks), that explains the deeper CO_2 sink. The duration of the bloom above the Kerguelen Plateau is due to iron fertilization but also due to the concomitant supply of major nutrients. Most investigations carried out in artificial blooms were limited to a few weeks, but in the case of SOIREE, satellite images show that the bloom was maintained over a longer time period (Abraham et al., 2000). This was likely due to a combination of iron regeneration within the bloom and nutrient supply from the surrounding waters. How deep the CO_2 sink was during the late phase of the artificial blooms is unknown.

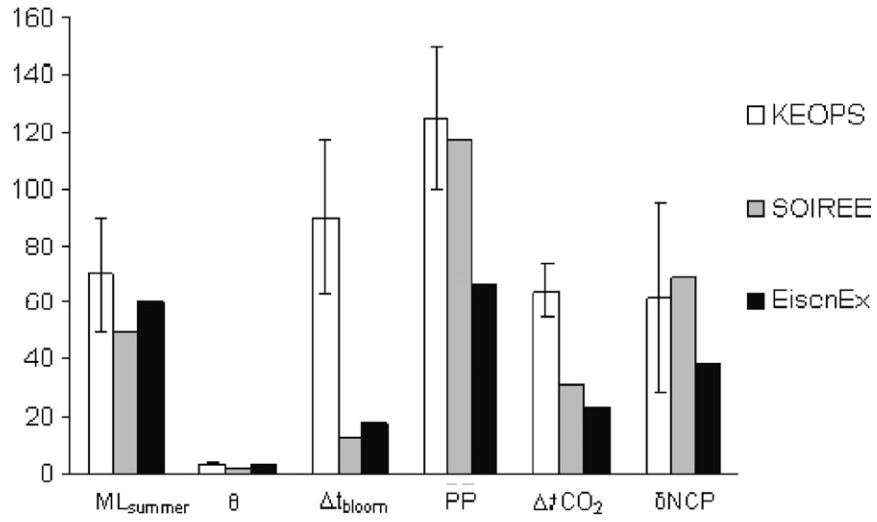

Fig. 4. Comparison of natural and artificial iron-fertilization experiments for several key parameters. ML_{summer} (m) is the depth of the mixed-layer temperature. θ (°C), is the temperature of the mixed layer. Δt_{bloom} (D) is the duration of the bloom for KEOPS and the duration of the period of observation for the artificial fertilization experiments. PP is the maximum of primary production (mmol m^{-2} d^{-1}). ΔfCO_2 (μatm) is the air–sea fCO_2 difference at A3 station. δNCP_{daily} (mmol m^{-2} d^{-1}) is the difference between A3 and C11 for KEOPS and between inside and outside the patch for the artificial iron-fertilization experiments (Gall et al., 2001; Gervais et al., 2002; Bozec et al., 2004; Boyd, 2004; Bakker et al., 2005).

During artificial iron-enrichment experiments, the impact of fertilization on NCP_{daily} was estimated by comparing stocks and fluxes of carbon inside and outside the patch (Bakker et al., 2005). In the case of KEOPS, the same approach was used by comparing NCP_{daily} between A3 and C11 (Fig. 4). Whatever the mode, natural or artificial fertilization, similar NCP_{daily} are obtained. This is consistent with the observation that similar levels of phytoplankton biomass or primary production are reported for both types of fertilization experiments. However, it is important to keep in mind that the amount of iron used to obtain this result is considerably lower during natural fertilization (Blain et al., 2007, 2008).

3.5. Carbon export

On the seasonal scale, the carbon exported below the mixed-layer depth was calculated by subtracting the summer stocks of POC and DOC in the mixed layer from the NCP_{season}. The accumulation of particulate inorganic carbon (PIC) was not determined during the cruise. However, it can be inferred from the variation in TA corrected for the variation of alkalinity due to the formation of POC. The seasonal alkalinity change (ΔAlk) was calculated as the difference between the alkalinity in winter (i.e. alkalinity at the depth of the temperature minimum) and the summer alkalinity (i.e. mean alkalinity in the mixed layer during the cruise). The accumulation of PIC was computed as $2(\Delta Alk - \Delta NO_3)$ where ΔNO_3 is the seasonal consumption of nitrate. This term is less than 0.7% of the NCP_{season} and was thus neglected in the calculation of the carbon export.

$$C_{exp\cdot season} = NCP_{season} - \Delta POC - \Delta DOC \quad (12)$$

The seasonal export was 5.4 ± 1.9 and 1.7 ± 0.4 mol m^{-2} at A3 and C11, respectively. The $C_{exp\cdot season}$ determined at A3 is among the highest determined in the Southern Ocean. In the Ross Sea, the export in mid summer was nine fold lower (0.6 ± 1.4 mol m^{-2}) than at A3, mainly due to the accumulation of POC and DOC in the surface mixed layer during this period of the year (Sweeney et al., 2000). In late summer grazing activity increased, leading to the formation of fast sinking aggregates (Sweeney et al., 2000) and a maximum export of 3.8 ± 0.8 mol m^{-2} in autumn.

During KEOPS, the carbon export also was measured using the ^{234}Th deficit method (Savoye et al., 2008). This method integrates the flux over roughly 20 days, but the ^{234}Th-derived C export fluxes are reported as mean daily fluxes (Table 2). For comparison, we derived the daily carbon export flux from the NCP_{daily}, as follows:

$$C_{exp\cdot daily} = NCP_{daily} - \frac{\Delta POC}{\Delta t_{bloom}} - \frac{\Delta DOC}{\Delta t_{bloom}} \quad (13)$$

At A3 and C11, we calculated $C_{exp.daily}$ of 85 ± 33 mmol m^{-2} d^{-1} and of 23 ± 8 mmol m^{-2} d^{-1}, respectively. This is 3 and 2 times higher than the carbon export estimated from the ^{234}Th-derived method at these stations (Table 2).

The carbon budget approach to estimate the carbon export is conservative because it inherently records all export events, which occur over the season, both in the particulate and the dissolved form. The ^{234}Th-derived carbon export estimates the flux on time scales of weeks using the steady-state approach, and ~20 days at A3 and 10 days at C11 using the non-steady-state approach (Savoye et al., 2008). It relies also on the determination of the ratio of POC to ^{234}Th and does not take into account

Table 2
Daily carbon export (mmol $m^{-2} d^{-1}$) estimates with the carbon budget method and with the U–Th-deficit method

	Budget method[a]	U–Th method[b]
A3	85±33	24.4±19.7
C11	23±8	12.2±3.3
Excess	62±33	12.2

[a]Export calculated at the base of the mixed layer.
[b]Export calculated at 100 m.

DOC export. Therefore, it is not surprising that both approaches do not reach a perfect agreement. The ^{234}Th carbon export derived from the non steady state approach (Savoye et al., 2008) shows large variability and a C export as large as 38.4 mmol $m^{-2} d^{-1}$ was recorded between 3 and 12 February at A3. This C export event might be triggered by the decline of the bloom. However, one cannot rule out that similarly large events also occurred before the KEOPS cruise. Time series of satellite images (Mongin et al., 2008) suggest that the bloom might be pulsed due to internal wave activity, which also could favor pulsed C export.

DOC export is difficult to quantify. DOC concentrations decrease almost linearly with depth below the mixed layer at A3. We calculated a vertical gradient of -6.7×10^{-2} mmol m^{-4}, and based on the K_z determined for A3 we obtained a vertical diffusive flux of -1.9 mmol $m^{-2} d^{-1}$. We can compare this value with the daily accumulation rate of DOC above the plateau that is derived from the seasonal DOC accumulation (610 mmol m^{-2}). For consistency with other extrapolations made previously in this paper for F_{atm} and F_{vert}, we assume that the DOC accumulated linearly over the season. We obtain an accumulation of DOC of 13.5 mmol $m^{-2} d^{-1}$. This compares quite well with the DOC accumulation rate of 11.2 mmol $m^{-2} d^{-1}$ reported for the surface mixed layer of the Ross Sea (Carlson et al., 1998). It represents probably the upper limit because the accumulation of DOC is likely at its maximum at the end of the season. DOC export outside the plateau via horizontal mixing probably occurred, but this cannot be quantified. Overall, it appears that DOC export represented only a small fraction of the carbon export above the Kerguelen Plateau.

Comparison with literature results indicates that the KEOPS C_{exp} results are towards the high end of export estimates. Indeed, $C_{exp\cdot daily}$ determined within the bloom above the Kerguelen Plateau is close to the daily C export determined by Buesseler et al. (2001), 44±17 mmol $m^{-2} d^{-1}$ and Cochran et al. (2000), 85 mmol $m^{-2} d^{-1}$ in the Ross Sea Gyre. Our $C_{exp\cdot daily}$ at C11 is not statistically different from the C_{exp} of 13.7±6 mmol $m^{-2} d^{-1}$ determined near the Polar Front in the Pacific Ocean (Buesseler et al., 2001) and close to the upper limit of 39 mmol $m^{-2} d^{-1}$ north of the Weddell Sea (Rutgers van der Loeff et al., 1997).

Taking into an account the DOC contribution and the temporal variability of POC export, the C_{exp} derived from the ^{234}Th approach can probably be considered as a lower bound of the export and the carbon budget as an upper limit. It is important to keep in mind that whatever the method, the carbon export was 2 times higher in waters above the plateau than outside.

The comparison of carbon export during KEOPS with artificial iron-fertilization experiments is the most relevant if similar approaches are used to estimate this term. In most of the artificial experiments carbon export was derived using the ^{234Th}-deficit method. The comparison with KEOPS is discussed in Savoye et al. (2008). Carbon export derived from the carbon budget is only reported for the south patch of SOFEX (Coale et al., 2004). The deficit of DIC within the iron-mediated bloom, 17 days after the last iron injection, was corrected for gas exchange and for POC accumulation resulting in a carbon export of 10.5 mmol $m^{-2} d^{-1}$. This value agrees with findings of Buesseler et al. (2004) applying the ^{234}Th method and it is eight fold lower than the carbon export estimated for the KEOPS bloom by the seasonal budget. When the DIC budget from the south patch of SOFEX was corrected for patch dilution, the carbon export increased up to 31.5 mmol $m^{-2} d^{-1}$. This is 2.5-fold lower than the carbon export derived from the KEOPS carbon budget. This difference is very similar to that observed between the ^{234}Th-derived C_{exp} fluxes in both experiments (Savoye et al., 2008). The higher carbon export in combination with the lower iron supply (Blain et al., 2008) leads to a high efficiency for carbon sequestration of the Kerguelen bloom compared to artificial blooms (Blain et al., 2007).

Acknowledgments

We thank the captain and the crew of the R/V *Marion Dufresne*. This work was supported by the Institut National des Sciences de L'Univers (INSU) du Centre National de la Recherche Scientifique (CNRS), l'Institut Paul Emile Victor (IPEV). The OISO program is supported by INSU, IPEV and Institut Pierre Simon Laplace (IPSL). We express our warm thanks to A. Corbiere, C. Lo Monaco and D. Thuillier (LOCEAN/IPSL) for sharing CO_2 analysis onboard. We are grateful to D. Nerini and M. Baklouti for their help in computing the sensitivity analysis. The authors acknowledge the constructive comments by B. Delille and an anonymous reviewer.

Appendix A. Determination of DIC_{winter}

The seasonal carbon budget strongly depends on the seasonal DIC concentrations (winter versus summer, as defined in Eq. (1)) to estimate the seasonal DIC depletion, ΔC_{sdep}. For summer, the DIC concentrations in the mixed-layer (Fig. 3) were determined in the two contrasting regions investigated here, within the bloom (station A3 sampled several times) and in HNLC waters (station C11). The summer DIC concentrations in surface waters also were determined through semi-continuous measurements

during the cruise (Fig. 2B). On the other hand, the determination of the surface DIC concentration in winter is based on the assumption that it equals the concentration of DIC at the depth of minimum temperature (T_{min}). Although this assumption has been applied in several studies in the Southern Ocean (e.g., Ishii et al., 1998, 2002; Rubin et al., 1998) as well as in high latitudes of the North Pacific (e.g., Midorikawa et al., 2002), its validity has never been clearly demonstrated. In the region investigated during KEOPS, several cruises have been conducted in recent years during austral summer and winter (Jabaud-Jan et al., 2004; Metzl et al., 2006). These data could help to verify the winter DIC derived from summer data in the T_{min} layer. Here we focus on stations occupied several times at 50°40S–68°25E, south-west of Kerguelen. At this location, temperature and DIC vertical profiles in summer are very close to those observed during KEOPS (Fig. 3); they all reveal a well defined temperature minimum at depth, and homogeneous DIC concentrations in the mixed-layer in summer or winter (see for example profiles presented on Fig. 6 in Metzl et al., 2006). In order to synthesize the seasonal observations, we have plotted (Fig. A1) DIC concentrations versus temperature for four stations during austral summer (end-December to mid-January) and two stations conducted in winter (end-July and mid-August). This plot first reveals that in summer the temperature minimum varies from year to year (range 1.4–2.1 °C), but DIC concentrations in the T_{min} layer do not vary dramatically (2147–2160 μmol kg^{-1}; large-gray symbols in Fig. A1). The data also indicate that DIC concentrations (2147–2160 μmol kg^{-1}) in the T_{min} layer are about the same each year (1998, 1999, 2000, 2001) but always higher than DIC concentrations observed in August (2135–2140 μmol kg^{-1}). This would suggest that the winter-layer T_{min} assumption is not valid to infer winter DIC concentrations, as it would lead to high DIC values. However, the OISO winter cruises have been conducted in mid-winter (July–August) and it is expected that DIC was not reaching maximum concentrations during these cruises. Indeed it is well known that sea surface temperature decreases until end-September or mid-October in this region (Jeandel et al., 1998) and results from biogeochemical models do suggest that DIC reaches maximum concentration in September–October and not in August (Jabaud-Jan et al., 2004; Metzl et al., 2006). We also note that maximum concentrations of nutrients in late winter (September–October) were previously observed and simulated in this region (JGOFS/KERFIX observations; Jeandel et al., 1998; Pondaven et al., 1998). This indicates that August (mid-winter) is not representative of late-winter conditions and that DIC is still increasing in surface waters between August and late-September, mid-October. We thus expect that DIC concentrations in late-winter should be higher (by at least 10 μmol kg^{-1}) than observed in August (Fig. A2). The

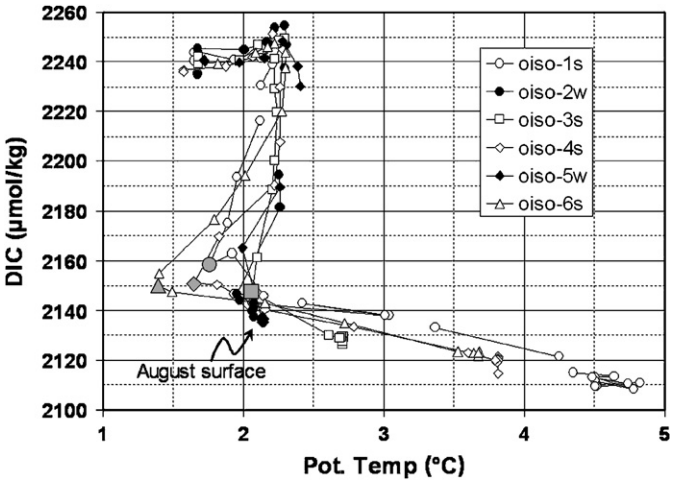

Fig. A1. DIC versus potential temperature from observations acquired during six OISO cruises (1998–2001) conducted at location 50°40S–68°25E (HNLC region southwest off Kerguelen Archipelago). Summer data (mid-December and January) are indicated by open symbols and the "s" notation at the end of the cruise number. Winter data (August) are indicated by filled symbols and the "w" notation at the end of cruise number. Large-gray symbols specify the DIC concentrations in the T_{min} winter layer as observed in summer.

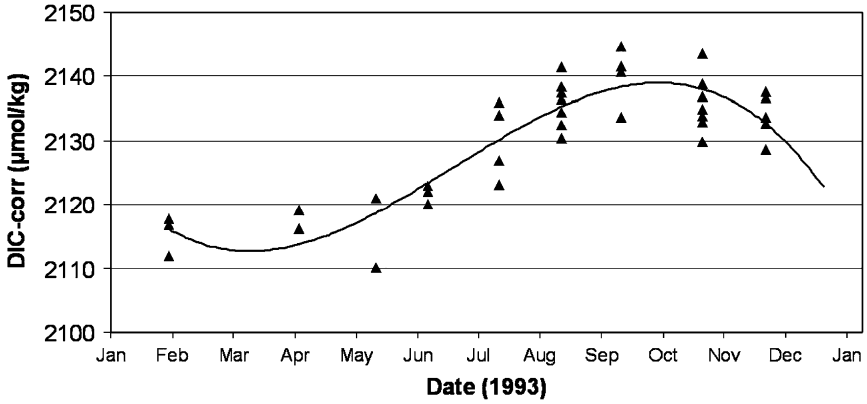

Fig. A2. DIC cycle in surface waters (10–40 m) observed in 1993 at the JGOFS/KERFIX station, 50°40S–68°25E, (Louanchi et al., 2001). DIC data from the original KERFIX data set (http://www.obs-vlfr.fr/cd_rom_dmtt/kfx_main.htm) have been corrected by −35 μmol kg^{-1} (Metzl et al., 2006). The annual DIC cycle constructed here suggests that maximum concentrations occurred in mid-September and are about 10 μmol kg^{-1} higher than in July–August.

comparison of seasonal profiles (Fig. A1) does not invalidate the method of winter values determination from measurement at $z_{T_{min}}$ during summer, but it points out the possible overestimate of DIC_{winter} by this method.

Appendix B. The carbon budget sensitivity analysis

The errors of all basic parameters involved in the carbon budget (DIC_{winter}, DIC_{summer}, $gradDIC_{80-150\,m}$, POC_{summer}, POC_{winter}, $z_{MLsummer}$, T, K_zA3 and K_zC11) are reported in Table 2. The mean NCP_{season}, NCP_{daily}, $C_{exp.season}$, $C_{exp\ daily}$ and associated uncertainties were computed using a global sensitivity analysis. This has been performed using a Monte Carlo method, the most widely used technique for global sensitivity analysis (Balakrishnan et al., 2005). Random values of each parameter were generated from probability distributions. Normal distribution (mean and standard deviation given in Table 1) were used for DIC_{winter}, DIC_{summer}, $gradDIC_{80-150\,m}$, POC_{summer}, POC_{winter}, ML_{summer} (C11), K_zC11. We made the assumption that the duration of the bloom could take any value between 60 and 120 days with the same probability. A uniform distribution was also used for K_z at C11 (with a minimum of $7.88\,m^2\,d^{-1}$ and a maximum of $48.23\,m^2\,d^{-1}$) and for F_{hor} at A3 (with a minimum of $0.01\,m^2\,d^{-1}$ and a maximum of $13\,m^2\,d^{-1}$). Considering the large standard deviation of K_z, $z_{MLsummer}$ at A3 and velocity coefficient for the whole area we chose to reconstruct the probability distribution for those parameters. The density of probability of $z_{MLsummer}$ were constructed from the experimental data set (16 and 40 data were used for K_z and $z_{MLsummer}$, respectively) according to the method of Silverman (1986). Density of velocity coefficient was estimated by a Weibull distribution with a set of 27 000 data. Based on 10^6 trial data we have then calculated the mean and the standard deviation of NCP_{season}, NCP_{daily}, $C_{exp\ season}$, $C_{exp\ daily}$.

References

Abraham, E.R., Law, C., Boyd, P.W., Lavender, S.J., Maldonado, M.T., Bowie, A.R., 2000. Importance of stirring in the development of an iron-fertilized phytoplankton bloom. Nature 407, 727–730.

Aristegui, J., Denis, M., Almunia, J., Montero, M.F., 2002. Water-column remineralization in the Indian sector of the Southern Ocean during early spring. Deep-Sea Research II 49, 1707–1720.

Aumont, O., Bopp, L., 2006. Globalizing results from ocean in situ iron fertilization studies. Global Biogeochemical Cycles 20, GB2017, doi:10.1029/2005GB002591.

Bakker, D.C.E., Bozec, Y., Nightingale, P.D., Goldson, L.E., Messias, M.J., De baar, H.J.W., Liddicoat, M.I., Skjelvan, I., Strass, V., Watson, A.J., 2005. Iron and mixing affect biological carbon uptake in soiree and EisenEx, two southern ocean iron fertilization experiments. Deep-Sea Research I 52, 1001–1019.

Balakrishnan, S., Roy, A., Ierapetritou, M.G., Flach, G.P., Georgopoulos, P.G., 2005. A comparative assessment of efficient uncertainty analysis techniques for environmental fate and transport models: application to the FACT model. Journal of Hydrology 307, 204–218.

Benner, R., Strom, M., 1993. A critical evaluation of the analytical blank associated with DOC measurements by high-temperature catalytic oxidation. Marine Chemistry 41, 153–160.

Blain, S., Tréguer, P., Belviso, S., Bucciarelli, E., Denis, M., Desabre, S., Fiala, M., Jézéquel, V.M., Lefèvre, M., Mayzaud, P., Marty, J.C., Razouls, S., 2001. A biogeochemical study of the island mass effect in the context of the iron hypothesis: Kerguelen Islands, Southern Ocean. Deep-Sea Research I 48, 163–187.

Blain, S., Quéguiner, B., Armand, L., Belviso, S., Bombled, B., Bopp, L., Bowie, A., Brunet, C., Brussaard, C., Carlotti, F., Christaki, U., Corbière, A., Durand, I., Ebersbach, F., Fuda, J.L., Garcia, N., Gerringa, L., Griffiths, B., Guigue, C., Guillerm, C., Jacquet, S., Jeandel, C., Laan, P., Lefèvre, D., Lomonaco, C., Malits, A., Mosseri, J., Obernosterer, I., Park, Y.-H., Picheral, M., Pondaven, P., Remenyi, T., Sandroni, V., Sarthou, G., Savoye, N., Scouarnec, L., Souhaut, M., Thuiller, D., Timmermans, K., Trull, T., Uitz, J., van-Beek, P., Veldhuis, M., Vincent, D., Viollier, E., Vong, L., Wagener, T., 2007. Impacts of natural iron fertilization on the Southern Ocean. Nature 446, 1070–1074.

Blain, S., Sarthou, G., Laan, P., 2008. Distribution of dissolved iron during the natural iron fertilisation experiment KEOPS (Kerguelen Plateau, Southern Ocean). Deep-Sea Research II, this issue [doi:10.1016/j.dsr2.2007.12.028].

Bopp, L., Kohfeld, K.E., Le Quéré, C., Aumont, O., 2003. Dust impact on marine biota and atmospheric CO_2 during glacial periods. Paleogeography 18.

Boyd, P., 2004. Ironing out algal issues in the Southern Ocean. Science 304, 396–397.

Boyd, P.W., Watson, A.J., Law, C.S., Abraham, E.R., Trull, T.W., Murdoch, R., Bakker, D.C.E., Bowie, A., Buesseler, K.O., Chang, H., Charette, M., Croot, P., Downing, K., Frew, R., Gall, M., Hadfield, M., Hall, J., Harvey, M., Jameson, G., LaRoche, J., Liddicoat, M., Ling, R., Maldonado, M.T., McKay, R.M., Nodder, S., Pickmere, S., Pridmore, R., Rintoul, S., Safi, K., Sutton, P., Strzepek, R., Tanneberger, K., Turner, S., Waite, A., Zeldis, J., 2000. A mesoscale phytoplankton bloom in the polar Southern Ocean stimulated by iron fertilization. Nature 407, 695–702.

Bozec, Y., Bakker, DC.E., Hartmann, C., Thomas, H., Bellerby, R.G.J., Nightingale, P.D., Riebesell, U., Watson, A.J., De Baar, H.J.W., 2004. The CO_2 system in a Redfield context during an iron enrichment experiment in the Southern Ocean. Marine Chemistry 95, 89–105.

Buesseler, K.O., Ball, L., Andrews, J., Cochran, J.K., Hirschberg, D.J., Bacon, M.P., Fleer, A., Brzezinski, M., 2001. Upper ocean export of particulate organic carbon and biogenic silica in the Southern Ocean along 170°W. Deep-Sea Research II 48, 4275–4297.

Buesseler, K.O., Andrews, J.E., Pike, S.M., Charette, M.A., 2004. The effects of iron fertilization on carbon sequestration in the Southern Ocean. Science 304, 414–417.

Carlson, C.A., Ducklow, H.W., Hansell, D.A., Smith, W.O., 1998. Organic carbon partitioning during spring phytoplankton blooms in the Ross Sea polynya and the Sargasso Sea. Limnology and Oceanography 43 (3), 275–386.

Charette, M.A., Buesseler, K.O., 2000. Does iron fertilization lead to a rapid export in the southern ocean? Geochemistry, Geophysics, Geosystems 1, 2000GC000069.

Coale, K.H., Johnson, K.S., Chavez, F.P., Buesseler, K.O., Barber, R.T., Brzezinski, M.A., Cochlan, W.P., Millero, F.J., Falkowski, P.G., Bauer, J.E., Wanninkhof, R.H., Kudela, R.M., Altabet, M.A., Hales, B.E., Takahashi, T., Landry, M.R., Bidigare, R.R., Wang, X., Chase, Z., Strutton, P.G., Friederich, G.E., Gorbunov, M.Y., Lance, V.P., Hilting, A.K., Hiscock, M.R., Demarest, M., Hiscock, W.T., Sullivan, K.F., Tanner, S.J., Gordon, R.M., Hunter, C.N., Elrod, V.A., Fitzwater, S.E., Jones, J.L., Tozzi, S., Koblizek, M., Roberts, A.E., Herndon, J., Brewster, J., Ladizinsky, N., Smith, G., Cooper, D., Timothy, D., Brown, S.L., Selph, K.E., Sheridan, C.C., Twining, B.S., Johnson, Z.I., 2004. Southern Ocean iron enrichment experiment: carbon cycling in high- and low-Si waters. Science 304, 408–414.

Cochran, J.K., Buesseler, K.O., Bacon, M.P., Wang, H.W., Hirschberg, D.J., Ball, L., Andrews, J., Crossin, G., Fleer, A., 2000. Short-lived thorium isotopes (^{234}Th, ^{228}Th) as indicators of POC export and particle cycling in the Ross Sea, Southern Ocean. Deep-Sea Research II 47, 3451–3490.

Copin-Montégut, C., 1988. A new formula for the effect of temperature on the partial pressure of CO_2 in seawater. Marine Chemistry 25, 29–37.

Copin-Montégut, C., 1989. A new formula for the effect of temperature on the partial pressure of CO_2 in seawater. Marine Chemistry 27, 143–144 (Corrigendum).

De Baar, H.J.W., de Jong, J.T.M., Bakker, D.C.E., Löscher, B.M., Veth, C., Bathmann, U., Smetacek, V., 1995. Importance of iron for plankton blooms and carbon dioxide drawdown in the Southern Ocean. Nature 373, 412–415.

De Baar, H.J.W., Boyd, P.W., Coale, K.H., Landry, M.R., Tsuda, A., Assmy, P., Bakker, D.C.E., Bozec, Y., Barber, R.T., Brzezinski, M.A., Buesseler, K.O., Boye, M., Croot, P.L., Gervais, F., Gorbunov, M.Y., Harrison, P.J., Hiscock, W.T., Laan, P., Lancelot, C., Law, C.S., Levasseur, M., Marchetti, A., Millero, F.J., Nishioka, J., Nojiri, Y., van Oijen, T., Riebesell, U., Rijkenberg, M.J.A., Saito, H., Takeda, S., Timmermans, K.R., Veldhuis, M.J.W., Waite, A.M., Wong, C-H., 2005. Synthesis of iron fertilization experiments: from the iron age in the age of enlightenment. Journal of Geophysical Research 110, 1–24.

Descolas-Gros, C., Mayzaud, P., 1997. MD102/ANTARES 3, Cruise report. Les Rapports des Campagnes à la mer, 97-2. Les publications de l'Institut Français pour la Recherche et la Technologie Polaires, 297pp.

Edmond, J.M., 1970. High precision determination of titration of alkalinity and total CO_2 of sea-water by potentiometric titration. Deep-Sea Research Oceanography (Abstract) 17, 737–750.

Gall, M.P., Strzepek, R., Maldonado, M., Boyd, P.W., 2001. Phytoplankton processes. Part 2: rates of primary production and factors controlling algal growth during the Southern Ocean Iron RElease Experiment (SOIREE). Deep-Sea Research II 48, 2571–2590.

Gervais, F., Riebesell, U., Gorbunov, M.Y., 2002. Changes in primary productivity and chlorophyll *a* in response to iron fertilization in the Southern Polar Frontal Zone. Limnology and Oceanography 47 (5), 1324–1335.

Gill, A.E., 1982. Atmosphere–Ocean Dynamics. Academic Press, New York, 662pp.

Ishii, M., Inoue, H.Y., Matsueda, H., Tanoue, E., 1998. Close coupling between seasonal biological production ad dynamics of dissolved inorganic carbon in the Indian Ocean sector and the western Pacific Ocean sector of the Antartic Ocean. Deep-Sea Research I 45, 1187–1209.

Ishii, M., Inoue, H.Y., Matsueda, H., 2002. Net community production in the marginal ice zone and its importance for the variability of the oceanic pCO_2 in the Southern Ocean south of Australia. Deep-Sea Research II 49, 1691–1706.

Jabaud-Jan, A., Metzl, N., Brunet, C., Poisson, A., Schauer, B., 2004. Interannual variability of the carbon dioxide system in the Southern Indian Ocean (20°S–60°S): the impact of a warm anomaly in austral summer 1998. Global Biogeochemical Cycles 18 (1), GB1042.

Jeandel, C., Ruiz-Pino, D., Gjata, E., Poisson, A., Brunet, C., Charriaud, E., et al., 1998. KERFIX, a permanent time-series station in the Southern Ocean: a presentation. Journal of Marine Systems 17, 555–569.

Jennings Jr., J.C., Gordon, L.I., Nelson, D.M., 1984. Nutrient depletion indicates high primary productivity in the Weddell Sea. Nature 309, 51–54.

Karl, D.M., Tilbrook, B.D., Tien, G., 1991. Seasonal coupling of organic matter production and particle flux in the western Brandsfield Strait, Antartica. Deep-Sea Research 38, 1097–1126.

Koertzinger, A., Mintrop, L., Wallace, D.W.R., Johnson, K.M., Neill, C., et al., 2000. The international at-sea intercomparison of fCO_2 systems during the R/V Meteor Cruise 36/1 in the North Atlantic Ocean. Marine Chemistry 2 (2-4), 171–192.

Lefèvre, D., Guigue, C., Obernosterer, I., 2008. The metabolic balance at two contrasting sites in the Southern Ocean: The iron-fertilized Kerguelen area and HNLC waters. Deep-Sea Research II, this issue [doi:10.1016/j.dsr2.2007.12.006].

Lo Monaco, C., Metzl, N., Poisson, A., Brunet, C., Schauer, B., 2005. Anthropogenic CO_2 in the Southern Ocean: distribution and inventory at the Indian–Atlantic boundary (World Ocean Circulation Experiment line I6). Journal of Geophysical Research 110, C06010.

Louanchi, F., Ruiz-Pino, D., Jeandel, C., Brunet, C., Schauer, B., et al., 2001. Dissolved inorganic carbon, alkalinity, nutrient and oxygen seasonal and interannual variations at the Antarctic Ocean JGOFS-KERFIX site. Deep-Sea Research I 48, 1581–1603.

Marinov, I., Gnanadesikan, A., Toggweiler, J.R., Sarmiento, J.L., 2006. The Southern Ocean biogeochemical divide. Nature 441, 964–967.

Metzl, N., Poisson, A., Louanchi, F., Brunet, C., Schauer, B., Brès, B., 1995. Spatio-temporal distributions of air–sea fluxes of CO_2 in the Indian and Antarctic Oceans: a first step. Tellus 47B, 56–69.

Metzl, N., Brunet, C., Jabaud-Jan, A., Poisson, A., Schauer, B., 2006. Summer and winter air–sea CO_2 fluxes in the Southern Ocean. Deep-Sea Research I 53, 1548–1563.

Midorikawa, T., Hiraishia, N., Ogawaa, K., Nemotoa, K., Kuboa, N., Ishii, M., 2002. Estimation of seasonal net community production and air–sea CO2 flux based on the carbon budget above the temperature minimum layer in the western subarctic North Pacific. Deep-Sea Research I 49, 339–362.

Mongin, M., Molina, E., Trull, T., 2008. Seasonality and scale of the Kerguelen Plateau phytoplankton bloom: a remote sensing and modeling analysis if the influence of natural iron fertilization in the Southern Ocean. Deep-Sea Research II, this issue [doi:10.1016/j.dsr2.2007.12.039].

Nightingale, P.D., Malin, G., Law, C.S., Watson, A.J., Liss, P.S., Liddicoat, M.I., Boutin, J., Upstill-Goddad, R.C., 2000. In-situ elevation of air sea gas exchange parametrisations using novel conservative and volatile tracers. Global Biogeochemical Cycles 14, 373–387.

Nodder, S.D., Charette, M.A., Waite, A.M., Trull, T.W., Boyd, P.W., Zeldis, J., Buesseler, K.O., 2001. Particle transformations and export flux during an *in situ* iron-stimulated bloom in the Southern Ocean. Geophysical Research Letters 28 (12), 2409–2412.

Park, Y.H., Fuda, J.L., Durand, I., Naveira Garabato, A.C., 2008. Internal tides and vertical mixing over the Kerguelen Plateau. Deep-Sea Research II, this issue [doi:10.1016/j.dsr2.2007.12.027].

Poisson, A., Metzl, N., Brunet, C., Schauer, B., Bres, B., Ruiz-Pino, R., Louanchi, F., 1993. Variability of sources and sinks of CO_2 and in the western Indian and Southern Oceans during the year 1991. Journal of Geophysical Research 98 (22), 759–778.

Pondaven, P., Fravalo, C., Ruiz-Pino, D., Tréguer, P., Quéguiner, B., Jeandel, C., 1998. Modelling the silica pump in the permanently open ocean zone of the Southern Ocean. Journal of Marine Systems 17, 587–619.

Price, J.F., Mooers, C.N.K., Van Leer, J.C., 1978. Observation and simulation of storm-induced mixed-layer deepening. Journal of Physical Oceanography 8, 582–599.

Roache, P.J., 1976. Computational Fluid Dynamics. Hermosa Press, Albuquerque, NM, USA, 446pp.

Rubin, S.I., Takahashi, T., Chipman, D.W., Goddard, J.G., 1998. Primary productivity and nutrient utilization ratios in the Pacific sector of the Southern Ocean based on seasonal changes in seawater chemistry. Deep-Sea Research I 45, 1211–1234.

Rutgers Van Der Loeff, M.M., Friedrich, J., Bathmann, U.V., 1997. Carbon export during the Spring Bloom at the Antarctic Polar Front, determined with the natural tracer ^{234}Th. Deep-Sea Research II 44, 457–478.

Sabine, C., Gruber, N., 2005. Response to comment on "The Ocean Sink for anthropogenic CO2". Science 308, [doi:10.1126/science.1109949].

Sarmiento, J.L., Gruber, N., Brzezinski, M.A., Dunne, J.P., 2004. High-latitude controls of thermocline nutrients and low-latitude biological productivity. Nature 427, 56–60.

Savoye, N., Trull, T.W., Jacquet, S., Navez, J., Dehairs, F., 2008. ^{234}Th-based export fluxes during a natural iron fertilisation experiment in the southern ocean (KEOPS). Deep-Sea Research II, this issue [doi:10.1016/j.dsr2.2007.12.036].

Sedwick, P.N., Di Tullio, G.R., 1997. Regulation of algal blooms in Antarctic shelf waters by the release of iron from melting sea ice. Geophysical Research Letters 24, 2515–2518.

Silverman, B.W., 1986. Density Estimation for Statistics and Data Analysis. Chapman & Hall, London.

Smetacek, V., 2001. EisenEx: international team conducts iron experiment in Southern Ocean. US JGOFS News 11 (1), 11–14.

Stammer, D., 1997. Global characteristics of ocean variability estimated from regional TOPEX/POSEIDON altimeter measurements. Journal of Physical Oceanography 27, 1743–1769.

Sweeney, C., Smith, W.O., Hales, B., Bidigare, R.R., Carlson, C.A., Codispoti, L.A., Gordon, L.I., Hansell, D.A., Millero, F.J., Park, M.O., Takahashi, T., 2000. Nutrient and carbon removal ratios and fluxes in the Ross Sea, Antarctica. Deep-Sea Research II 47, 3395–3421.

Wanninkhof, R., McGillis, W., 1999. A cubic relationship between air–sea CO_2 exchange and wind speed. Geophysical Research Letters 26, 1889–1892.

Watson, A.J., Naveiro Garabato, A.C., 2006. The role of Southern ocean mixing and up-welling in glacial–interglacial time atmospheric CO_2 change. Tellus 58B, 73–87.

Weiss, R.F., 1974. Carbon dioxide in water and seawater: the solubility of a non-ideal gas. Marine Chemistry 2, 203–215.

Weiss, R.F., Price, B.A., 1980. Nitrous oxide solubility in water and seawater. Marine Chemistry 8, 347–359.

Williams, P.J.LeB., 1993. On the definition of plankton production terms. ICES Marine Science Symposia 197, 9–19.